

Review of thermodynamic structures and structure-preserving discretisations of Cahn–Hilliard-type models

Aaron Brunk[✉], Marco F.P. ten Eikelder[✉], Marvin Fritz[✉], Dennis Höhn[✉], and Dennis Trautwein[✉]

Abstract The Cahn–Hilliard equation and extensions, notably the Cahn–Hilliard–Darcy and Cahn–Hilliard–Navier–Stokes systems, provide widely used frameworks for coupling interfacial thermodynamics with flow. This review surveys the thermodynamic structures underlying these models, focusing on the formulation of free energy functionals, dissipation mechanisms, and variational principles. We compare structural properties, emphasizing how these models encode conservation laws and energy dissipation. A central theme is the translation of these thermodynamic structures into numerical practice by providing representative discretisation strategies that aim to preserve mass conservation, stability, and energy decay. Particular attention is paid to the trade-offs between accuracy, efficiency, and structure preservation in large-scale simulations.

1 Introduction

Phase-field models have become a cornerstone in the mathematical description of multiphase systems, with the Cahn–Hilliard (CH) equation and its extensions serving as prototypical examples; we refer to the review articles [23, 26, 29, 47, 55, 69] and the references therein. These models couple thermodynamic consistency with interfacial dynamics and, when combined with fluid flow, give rise to the Cahn–Hilliard–Darcy

Aaron Brunk
Johannes Gutenberg University Mainz, e-mail: abrunk@uni-mainz.de

Marco F.P. ten Eikelder
Technical University of Darmstadt, e-mail: marco.eikelder@tu-darmstadt.de

Marvin Fritz
Radon Institute for Computational and Applied Mathematics, e-mail: marvin.fritz@oeaw.ac.at

Dennis Höhn
Johannes Gutenberg University Mainz, e-mail: dennis.hoehn@uni-mainz.de

Dennis Trautwein
University of Regensburg, e-mail: dennis.trautwein@ur.de

(CHD) and Cahn–Hilliard–Navier–Stokes (CHNS) systems. A unifying feature of such models is the presence of underlying thermodynamic structures, notably conservation laws and energy dissipation, which are essential for both physical interpretability and long-time stability.

Transferring these structures to the discrete setting has been the subject of extensive research, leading to the development of structure-preserving numerical schemes. Such methods aim to retain key properties such as mass conservation and energy decay, thereby providing more reliable simulations than conventional discretisations. This survey highlights the thermodynamic framework underlying CH-type models, reviews representative discretisation strategies, and discusses the trade-offs between accuracy, efficiency, and structure preservation. The emphasis is on presenting common structural principles and illustrating how they inform the design of robust numerical methods.

Beyond the CH, CHD, and CHNS systems considered here, structure-preserving methods have been studied for Cahn–Hilliard type models coupled with Biot’s equation [15], nonlocal interactions [13], magnetohydrodynamics [62], Poisson–Nernst–Planck dynamics [58], reaction–diffusion systems [66], Forchheimer’s equation [14] and lymphangiogenesis models [44, 65].

2 Models

The mixed forms of the Cahn–Hilliard type models read:

Cahn–Hilliard (CH) system

$$\partial_t \phi - \operatorname{div}(m(\phi) \nabla \mu) = 0, \quad \mu + \gamma \Delta \phi - f'(\phi) = 0 \quad (1)$$

Cahn–Hilliard–Darcy (CHD) system

$$\partial_t \phi + \operatorname{div}(\phi \mathbf{v}) - \operatorname{div}(m(\phi) \nabla \mu) = 0, \quad \mu + \gamma \Delta \phi - f'(\phi) = 0, \quad (2a)$$

$$\alpha(\phi) \mathbf{v} + \nabla p + \operatorname{div}(\gamma \nabla \phi \otimes \nabla \phi) = 0, \quad \operatorname{div}(\mathbf{v}) = 0, \quad (2b)$$

Cahn–Hilliard–Navier–Stokes (CHNS) system

$$\partial_t \phi + \operatorname{div}(\phi \mathbf{v}) - \operatorname{div}(m(\phi) \nabla \mu) = 0, \quad \mu + \gamma \Delta \phi - f'(\phi) = 0, \quad (3a)$$

$$\partial_t \mathbf{v} + \operatorname{div}(\mathbf{v} \otimes \mathbf{v}) - \operatorname{div}(\eta(\phi) \mathbf{D} \mathbf{v}) + \nabla p + \operatorname{div}(\gamma \nabla \phi \otimes \nabla \phi) = 0, \quad \operatorname{div}(\mathbf{v}) = 0, \quad (3b)$$

in domain $\Omega \subset \mathbb{R}^d$ (dimension $d = 2, 3$). In these models, $\phi \in [0, 1]$ denotes the phase field variable, which represents an order parameter (e.g. volume fraction, mass fraction or concentration), μ is the chemical potential, \mathbf{v} is the mixture velocity, and p is the Lagrange multiplier pressure. Furthermore, $m = m(\phi)$ is the mobility function, $f = f(\phi)$ is the gradient-free part of the Helmholtz free energy density, γ is a parameter related to the interfacial width, and $\eta = \eta(\phi)$ is the viscosity. The CH equation is a diffuse interface model for phase separation in binary mixtures. It evolves an order parameter that captures spinodal decomposition and coarsening (Eq. (1)). The CHD model describes a system that involves both phase separation/coarsening (Eq. (2a)) and porous medium flow (Eq. (2b)). The CHNS system models phase separation (Eq. (3a))

and incompressible hydrodynamics (Eq. (3b)). The systems have to be complemented by boundary and initial conditions. In this review, we consider for simplicity periodic boundary conditions. From a physical perspective, the CHNS system is the most complete model of these three. In certain regimes where inertia is not dominant, certain model reductions/approximations, like the CHD system, appear to be valid. Whenever the momentum is negligible, the standard Cahn–Hilliard system is a suitable reduction.

We proceed with the physical structures encoded in these systems. We define the mass, linear momentum, angular momentum, and energy, respectively, as:

$$M = \int_{\Omega} \phi \, dx, \quad \mathbf{L} = \int_{\Omega} \mathbf{v} \, dx, \quad \mathbf{P} = \int_{\Omega} \mathbf{v} \times \mathbf{x} \, dx, \quad E_{\beta} = \int_{\Omega} \Psi + \frac{\beta}{2} |\mathbf{v}|^2 \, dx,$$

where the free energy density is $\Psi = \frac{\gamma}{2} |\nabla \phi|^2 + f(\phi)$, and where $\beta = 0$ for CH and CHD, and $\beta = 1$ for CHNS. In Table 1, we summarise the conservation and dissipation structures of the models.

Model	Structure	Formula
CH	Mass conservation	$\frac{d}{dt} M = 0$
	Energy dissipation	$\frac{d}{dt} E_0 = -\langle m(\phi) \nabla \mu, \nabla \mu \rangle \leq 0$
CHD	Mass conservation	$\frac{d}{dt} M = 0$
	Energy dissipation	$\frac{d}{dt} E_0 = -\langle \alpha(\phi) \mathbf{v}, \mathbf{v} \rangle - \langle m(\phi) \nabla \mu, \nabla \mu \rangle \leq 0$
CHNS	Mass conservation	$\frac{d}{dt} M = 0$
	Linear/angular momentum cons.	$\frac{d}{dt} \mathbf{L} = 0 \quad \frac{d}{dt} \mathbf{P} = 0$
	Energy dissipation	$\frac{d}{dt} E_1 = -\langle m(\phi) \nabla \mu, \nabla \mu \rangle - \langle \eta(\phi) \nabla \mathbf{v}, \nabla \mathbf{v} \rangle \leq 0$

Table 1: Physical structures for CH, CHD, and CHNS.

The mass conservation equations follow from the integration of the phase-field equation over Ω , subsequently integrating by parts, and applying the periodic boundary conditions. Next, linear and angular momentum conservation in the CHNS model follows analogously as in the classical Navier-Stokes equations, see e.g. a standard textbook on continuum mechanics such as [64]. Finally, the energy-dissipation laws result from choosing the appropriate weights, taking the superposition, and integrating. The weights are μ for the ϕ equation, $-\partial_t \phi$ for the μ , \mathbf{v} for the \mathbf{v} equation and p for the divergence equation. We note that to establish the energy-dissipation law of CHD/CHNS, we used the following identity for the Korteweg stress $\text{div}(\gamma \nabla \phi \otimes \nabla \phi) = \nabla \Psi - \mu \nabla \phi$.

3 Discretisation

We assume that $\Omega \subset \mathbb{R}^d$ is a convex polyhedral domain and \mathcal{T}_h is assumed to be a globally quasi-uniform triangulation of Ω . The phase-field and its chemical potential are discretised by continuous piece-wise linear elements, while for velocity-pressure we

use standard LBB stable spaces; e.g. Taylor–Hood elements, see [10] for further details. We denote by $\mathbb{P}_k = \{v \in L^2(\Omega) : v|_K \in \mathbb{P}_k(K) \forall K \in \mathcal{T}_h\}$ the finite element space of piecewise polynomials of degree k , and by $\mathbb{P}_k^c = \{v \in H^1(\Omega) : v|_K \in \mathbb{P}_k(K) \forall K \in \mathcal{T}_h\}$ the globally continuous version. We choose the spaces

$$\begin{aligned}\mathcal{V}_h &:= \mathbb{P}_1^c, & X_h &:= (\mathbb{P}_2^c)^d, & Q_h &:= \mathbb{P}_1^c, & \mathcal{W}_h &:= \mathbb{P}_1 \\ \mathcal{Z}_h &:= \{\mathbf{v} \in [L^2(\Omega)]^d : \nabla \cdot \mathbf{v} \in L^2(\Omega), \mathbf{v}|_K \in [\mathbb{P}_2(K)]^d \forall K \in \mathcal{T}_h\}.\end{aligned}$$

We divide the time interval $[0, T]$, $T > 0$ fixed, into uniform steps with step size $\tau > 0$ and introduce $\mathcal{I}_\tau := \{0 = t^0, t^1 = \tau, \dots, t^{n_T} = T\}$, where $n_T = \frac{T}{\tau}$ is the absolute number of time steps. We denote by $\Pi_c^1(\mathcal{I}_\tau; X)$ and $\Pi^0(\mathcal{I}_\tau; X)$ the spaces of continuous piecewise linear and piecewise constant functions on \mathcal{I}_τ with values in the space X , respectively. By g^{n+1} and g^n we denote the evaluation of a function g in $\Pi_c^1(\mathcal{I}_\tau; X)$ or $\Pi^0(\mathcal{I}_\tau; X)$ at $t = \{t^{n+1}, t^n\}$, respectively, and write $I_n = (t^n, t^{n+1})$. The discrete-time derivative is denoted by $d_\tau^{n+1} g := \frac{g^{n+1} - g^n}{\tau}$. We note that we use the time-averaged method to approximate the potential derivative, that is,

$$f'(\phi^{n+1}, \phi^n) := \frac{1}{\tau} \int_{t^n}^{t^{n+1}} f'(\phi_{\text{avg}}^{n,n+1}(s)) ds, \quad \phi_{\text{avg}}^{n,n+1}(s) = \frac{\phi^{n+1} - \phi^n}{\tau}(s - t^n) + \phi^n.$$

We briefly remark on the above choice of time integration of the potential derivative. In general the double-well potential considered for Cahn–Hilliard systems are neither convex nor concave. Hence, low-order methods like implicit or explicit Euler fail to be unconditionally energy-stable, [61]. Conditional stability can be achieved using structural assumption on the potential. However, such restrictions are unfavoured latest when considering long-time simulations. In the lowest order case unconditional stability can be achieved using convex-concave decomposition or stabilised methods and similar extensions for higher-order methods [32, 38, 61]. Both methods introduce numerical diffusion in time. Our approach utilises exact integration in time and hence no numerical diffusion is introduced. The method is quite similar to the averaged vector-field method [33, 50].

3.1 Cahn–Hilliard system

Let $\phi_h^0 \in \mathcal{V}_h$ be given; seek functions $(\phi_h, \mu_h) \in \Pi_c^1(\mathcal{I}_\tau; \mathcal{V}_h) \times \Pi^0(\mathcal{I}_\tau; \mathcal{V}_h)$ such that

$$\langle d_\tau^{n+1} \phi_h, \psi_h \rangle + \langle m(\phi_h^{n+1}) \nabla \mu_h^{n+1}, \nabla \psi_h \rangle = 0, \quad (5)$$

$$\langle \mu_h^{n+1}, \xi_h \rangle - \gamma \langle \nabla \phi_h^{n+1}, \nabla \xi_h \rangle - \langle f'(\phi_h^{n+1}, \phi_h^n), \xi_h \rangle = 0, \quad (6)$$

holds for all $(\psi_h, \xi_h) \in \mathcal{V}_h \times \mathcal{V}_h$ and for all $0 \leq n < n_T$. This scheme is fully implicit in the interfacial terms, uses a time-averaged treatment of the bulk potential, and yields a discrete energy law mirroring the continuous one (see Theorem 1).

We note that a broad variety of structure-preserving discretisations have been developed for CH to guarantee (at least) energy stability. Discontinuous Galerkin

schemes have been proposed, see [2, 67], as well as upwind-based SAV (Scalar Auxiliary Variable) approaches [43]. Energy-stable formulations with dynamic boundary conditions are studied in [30, 56, 57], while further SAV-type schemes have been analysed in, e.g., [52–54]. The CH equation has also been reformulated in a port-Hamiltonian framework [4, 9], and more recently, machine-learning-based discretisations with built-in structure preservation have been explored [19]. Anisotropic variants have been addressed in [49], while optimization-based reformulations lead to alternative stable discretisations [22]. Finite volume schemes with unconditional energy stability are developed and analysed in [6, 7].

Beyond energy-stable schemes, there are other structures of interest that one could try to preserve. We mention the bound preserving property such as $\phi_h \in [0, 1]$ when considering degenerate mobilities and singular potentials, see [6, 8, 24]. Furthermore, one may prove the attainment of a steady-state, which is true for the continuous model (see [1, 59]), and it was shown in [5, 11, 51] for several discretisation schemes.

3.2 Cahn–Hilliard–Darcy system

Let $\phi_h^0 \in \mathcal{V}_h$ be given; seek function $\phi_h \in \Pi_c^1(\mathcal{I}_\tau; \mathcal{V}_h)$ and $(\mu_h, \mathbf{v}_h, p_h) \in \Pi^0(\mathcal{I}_\tau; \mathcal{V}_h \times \mathcal{Z}_h \times \mathcal{W}_h)$ such that

$$\langle d_\tau^{n+1} \phi_h, \psi_h \rangle - \langle \phi_h^{n+1} \mathbf{v}_h^{n+1}, \nabla \psi_h \rangle + \langle m(\phi_h^{n+1}) \nabla \mu_h^{n+1}, \nabla \psi_h \rangle = 0, \quad (7)$$

$$\langle \mu_h^{n+1}, \xi_h \rangle - \gamma \langle \nabla \phi_h^{n+1}, \nabla \xi_h \rangle - \langle f'(\phi_h^{n+1}, \phi_h^n), \xi_h \rangle = 0, \quad (8)$$

$$\langle \alpha(\phi_h^{n+1}) \mathbf{v}_h^{n+1}, \mathbf{w}_h \rangle - \langle p_h^{n+1}, \operatorname{div}(\mathbf{w}_h) \rangle + \langle \phi_h^{n+1} \nabla \mu_h^{n+1}, \mathbf{w}_h \rangle = 0, \quad (9)$$

$$\langle \operatorname{div}(\mathbf{v}_h^{n+1}), q_h \rangle = 0 \quad (10)$$

holds for all $(\psi_h, \xi_h, \mathbf{w}_h, q_h) \in \mathcal{V}_h \times \mathcal{Z}_h \times \mathcal{W}_h$ and for all $0 \leq n < n_T$.

Similar to the classical CH equation, a broad variety of structure-preserving discretisations have been developed for the CHD system and related variants. Several finite element schemes achieve first- or second-order temporal accuracy, while maintaining energy stability and often allowing decoupled solution strategies [40, 41, 72]. An energy-stable and well-posed FE scheme was also proposed for the related CH–Forchheimer system [14]. Other FE-based studies provide energy-stable approximations and error estimates for CHD models with additional Stokes-type stabilisation terms [18, 21]. Alternative SAV formulations yield linear, unconditionally energy-stable schemes for CHD systems [70, 71, 73]. In the context of finite difference methods, both first- and second-order time-accurate energy-stable schemes have been constructed and analysed [17, 68]. A rigorous analytical framework for the CHD system and its finite element approximation was established in [28], confirming the continuous and discrete energy dissipation properties. Finally, a local DG method was proposed in [39], which also preserves a discrete energy law while offering flexibility for complex geometries.

3.3 Cahn–Hilliard–Navier–Stokes system

Let $(\phi_h^0, \mathbf{v}_h^0) \in \mathcal{V}_h \times \mathcal{X}_h$ be given. We seek function $(\phi_h, \mathbf{v}_h) \in \Pi_c^1(\mathcal{I}_\tau; \mathcal{V}_h \times \mathcal{X}_h)$ and $(\mu_h, p_h) \in \Pi^0(\mathcal{I}_\tau; \mathcal{V}_h \times \mathcal{Q}_h)$ such that

$$\langle d_\tau^{n+1} \phi_h, \psi_h \rangle - \langle \phi_h^{n+1} \mathbf{v}_h^{n+1}, \nabla \psi_h \rangle + \langle m(\phi_h^{n+1}) \nabla \mu_h^{n+1}, \nabla \psi_h \rangle = 0, \quad (11)$$

$$\langle \mu_h^{n+1}, \xi_h \rangle - \gamma \langle \nabla \phi_h^{n+1}, \nabla \xi_h \rangle - \langle f'(\phi_h^{n+1}, \phi_h^n), \xi_h \rangle = 0, \quad (12)$$

$$\begin{aligned} \langle d_\tau^{n+1} \mathbf{v}_h, \mathbf{w}_h \rangle + \mathbf{c}_{skw}(\mathbf{v}_h^{n+1}, \mathbf{v}_h^{n+1}, \mathbf{w}_h) + \langle \eta(\phi_h^{n+1}) \mathbf{D} \mathbf{v}_h^{n+1}, \mathbf{D} \mathbf{w}_h \rangle \\ - \langle p_h^{n+1}, \operatorname{div}(\mathbf{w}_h) \rangle + \langle \phi_h^{n+1} \nabla \mu_h^{n+1}, \mathbf{w}_h \rangle = 0, \end{aligned} \quad (13)$$

$$\langle \operatorname{div}(\mathbf{v}_h^{n+1}), q_h \rangle = 0 \quad (14)$$

holds for all $(\psi_h, \xi_h, \mathbf{w}_h, q_h) \in \mathcal{V}_h \times \mathcal{V}_h \times \mathcal{X}_h \times \mathcal{Q}_h$ and for all $0 \leq n < n_T$. Here we used the skew-symmetric form

$$\mathbf{c}_{skw}(\mathbf{v}_h^*, \mathbf{v}_h^{n+1}, \mathbf{w}_h) := \frac{1}{2} \langle (\mathbf{v}_h^* \cdot \nabla) \mathbf{v}_h^{n+1}, \mathbf{w}_h \rangle - \frac{1}{2} \langle (\mathbf{v}_h^* \cdot \nabla) \mathbf{w}_h, \mathbf{v}_h^{n+1} \rangle.$$

Similarly to CH and CHD, a growing body of work develops structure-preserving discretisations for the CHNS system. For the case of matching densities, energy-stable methods are proposed in e.g. [20, 27, 45, 48]. For the case of non-matching densities modelled via quasi-incompressible models, we mention a nonlinear discontinuous Galerkin energy-stable discretisation [31], a linear conditionally energy-stable continuous Galerkin method [63], an unconditionally energy-stable nonlinear continuous Galerkin method [12], and a divergence-conforming discretisation [25]. Furthermore, the works [3, 37] propose methods that are both energy-stable and provide bounds on the phase-field parameter. The related Abels–Garcke–Grün model was studied in [16, 34–36] with respect to an energy-stable and or positivity-preserving scheme. Finally, we note the work of Hong et al. [42] that provides a physics-informed, structure-preserving numerical scheme for ternary hydrodynamics, and the work of Khanwale et al. [46] for a discretisation of CHNS for turbulence.

3.4 Mass balance and energy dissipation

Theorem 1 *Solutions of all schemes conserve mass $\langle \phi_h^{n+1}, 1 \rangle = \langle \phi_h^n, 1 \rangle$.*

CH: *Every discrete solution of scheme (5)–(6) satisfies*

$$E_0(\phi_h^{n+1}) + \tau \langle m(\phi_h^{n+1}) \nabla \mu_h^{n+1}, \nabla \mu_h^{n+1} \rangle \leq E_0(\phi_h^n).$$

CHD: *Every discrete solution of scheme (7)–(10) satisfies*

$$E_0(\phi_h^{n+1}) + \tau \langle m(\phi_h^{n+1}) \nabla \mu_h^{n+1}, \nabla \mu_h^{n+1} \rangle + \tau \langle \alpha(\phi_h^{n+1}) \mathbf{v}_h^{n+1}, \mathbf{v}_h^{n+1} \rangle \leq E_0(\phi_h^n).$$

CHNS: *Every discrete solution of scheme (11)–(14) satisfies*

$$E_1(\phi_h^{n+1} \mathbf{v}_h^{n+1}) + \tau \langle m(\phi_h^{n+1}) \nabla \mu_h^{n+1}, \nabla \mu_h^{n+1} \rangle + \tau \langle \eta(\phi_h^{n+1}) \mathbf{D} \mathbf{v}_h^{n+1}, \mathbf{D} \mathbf{v}_h^{n+1} \rangle \leq E_1(\phi_h^n, \mathbf{v}_h^n).$$

Proof. Mass conservation follows from $\psi_h = 1$. For the energy we use $(a^2 - b^2) = 2(a, a - b) - (a - b)^2$ compute

$$\begin{aligned} \frac{1}{\tau}(E_\beta(\phi_h^{n+1}, \mathbf{v}_h^{n+1}) - E_\beta(\phi_h^n, \mathbf{v}_h^n)) &= \gamma \langle \nabla \phi_h^{n+1}, \nabla d_\tau^{n+1} \phi_h \rangle + \beta \langle d_\tau^{n+1} \mathbf{v}_h, \mathbf{v}_h^{n+1} \rangle \\ &\quad - \frac{\tau \gamma}{2} \|d_\tau^{n+1} \nabla \phi_h\|_{L^2}^2 - \frac{\tau \beta}{2} \|d_\tau^{n+1} \mathbf{v}_h\|_{L^2}^2 \\ &\quad + \frac{1}{\tau} \langle f(\phi_h^{n+1}) - f(\phi_h^n), 1 \rangle \end{aligned}$$

The second line can be estimated by zero and for the third line we use mean-value theorem to obtain

$$\begin{aligned} \frac{1}{\tau} \langle f(\phi_h^{n+1}) - f(\phi_h^n), 1 \rangle &= \frac{1}{\tau} \int_{t^n}^{t^{n+1}} \partial_t f(\phi_{h,\text{avg}}^{n,n+1}(s)) ds \\ &= \frac{1}{\tau} \int_{t^n}^{t^{n+1}} f'(\phi_{h,\text{avg}}^{n,n+1}(s)) \partial_t \phi_{h,\text{avg}}^{n,n+1}(s) ds \\ &= \left\langle \frac{1}{\tau} \int_{t^n}^{t^{n+1}} f'(\phi_{h,\text{avg}}^{n,n+1}(s)) ds, d_\tau^{n+1} \phi_h \right\rangle \\ &= \langle f'(\phi_h^{n+1}, \phi_h^n), d_\tau^{n+1} \phi_h \rangle \end{aligned}$$

Using $\xi_h = d_\tau^{n+1} \phi_h$, we obtain:

$$\frac{1}{\tau}(E_\beta(\phi_h^{n+1}, \mathbf{v}_h^{n+1}) - E_\beta(\phi_h^n, \mathbf{v}_h^n)) \leq \langle d_\tau^{n+1} \phi_h, \mu_h^{n+1} \rangle + \beta \langle d_\tau^{n+1} \mathbf{v}_h, \mathbf{v}_h^{n+1} \rangle$$

cf. [12–14], the energy inequalities follow from the same test function as at the continuous level. \square

4 Experiments

The schemes of the previous section are implemented in NGSolve [60]. The nonlinear system is treated using Newton’s method with an absolute tolerance of 10^{-11} , while the linear system is solved by a direct solver. We consider the two-dimensional domain $\Omega = (0, 1)^2$. In the experiments, we fix $\gamma = 10^{-4}$, $h = 10^{-2}$, $\tau = 10^{-3}$ and use the following functions that appear in the models:

$$\begin{aligned} f(\phi) &= \frac{1}{4} \phi^2 (1 - \phi)^2, & m(\phi) &= 5 \max\{\phi^2 (1 - \phi)^2, 0\} + 10^{-6}, \\ \alpha(\phi) &= \exp(\phi \ln(\alpha_1) + (1 - \phi) \ln(\alpha_0)), & \eta(\phi) &= \exp(\phi \ln(\eta_1) + (1 - \phi) \ln(\eta_0)), \end{aligned}$$

where $\alpha_1 = 1$, $\alpha_0 = 10^{-2}$, $\eta_1 = 10^{-2}$, $\eta_0 = 10^{-4}$. We consider the following initial data:

$$\phi_0(x, y) = 0.4 + \mathcal{U}(x, y), \quad \mathcal{U}(x, y) \in [-10^{-3}, 10^{-3}], \quad \mathbf{v}_0(x, y) = (0, 0)^\top.$$

In Figure 1, we compare the temporal evolution of all three models. Until $t = 0.3$, all three models produce very similar solutions, corresponding to the stage in which the relevant interfaces have formed. At this point, CH relies solely on diffusive dynamics of the droplets, whereas the velocity-dependent models introduce additional transport effects, which in this case accelerate the phase separation.

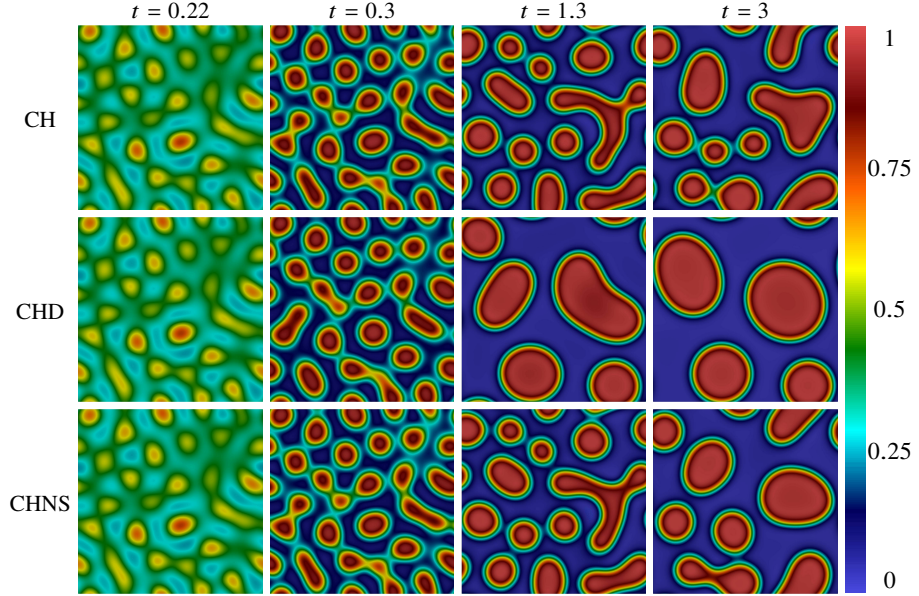


Fig. 1: Snapshots of ϕ for CH, CHD, CHNS from top to bottom.

In Figure 2, we compare the temporal evolution of the energy and the mass conservation error. As predicted by Theorem 1, the conservation of mass holds up to machine accuracy, while the energy is dissipative. It is shown in Figure 2 that the energy of the CHNS model in the final stages is lower than that of the CH model, although there is a non-zero contribution of kinetic energy. Remarkably, the CHD system drives the phase separation much faster, such that even at $t = 1.3$ the process is significantly more advanced than in the other two models at $t = 3$. It is important to recall that the velocity field is induced by the phase-field through the Korteweg stress.

In Figure 3, we compare the local divergence error, that is, $\|\nabla \cdot \mathbf{v}\|_{L^2}$, as well as the linear and angular momentum errors for CHNS. We observe that the divergence error remains in machine precision for CHD, while for CHNS it levels around 10^{-6} . This behaviour is expected: CHD discretisation admits the choice $q_h = \nabla \cdot \mathbf{v}_h$, enforcing the freedom of local divergence, while CHNS discretisation does not, and thus it is not locally divergence free. Furthermore, linear and angular momentum are not preserved in CHNS, since the scheme is not designed to conserve them.

Acknowledgements The work of A.B. was supported by the Deutsche Forschungsgemeinschaft (DFG) via TRR 146, project number 233630050 and together with D.H. via SPP 2256 project number 441153493. MtE was supported by the DFG via project EI 1210/5-1, number 566600860. The author

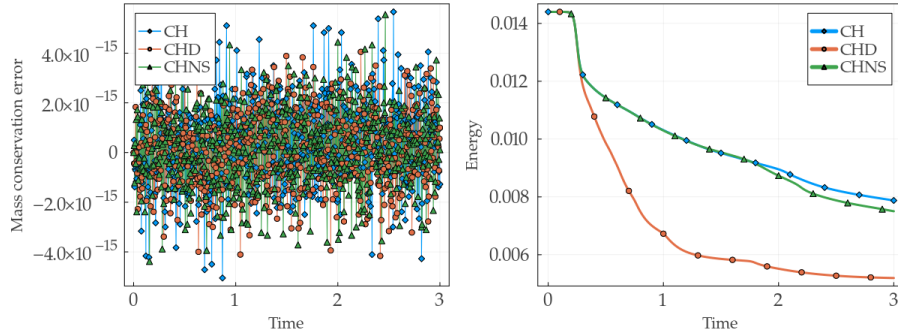


Fig. 2: Comparison of mass conservation and energy evolution for CH, CHNS, CHD.

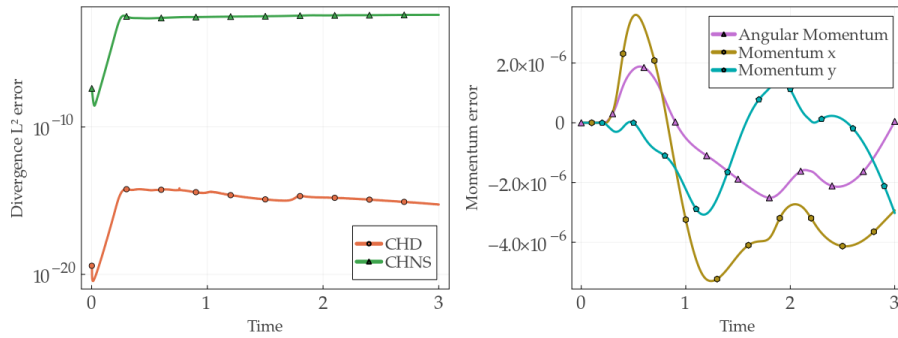


Fig. 3: Comparison of local divergence-freedom for CHD and CHNS on logarithmic scale (left) and conservation errors of linear and angular momentum for CHNS (right).

M.F. is supported by the State of Upper Austria. D.T. was supported by the DFG through the Gradiertenkolleg 2339 IntComSin (Project-ID 321821685), and by the Swedish Research Council (grant no. 2021-06594) during his stay at Institut Mittag-Leffler, Sweden, in 2025.

References

1. Abels, H., Wilke, M.: Convergence to equilibrium for the Cahn–Hilliard equation with a logarithmic free energy. *Nonlinear Anal.-Theor.* **67**(11), 3176–3193 (2007)
2. Acosta-Soba, D., Guillén-González, F., Rodríguez-Galván, J.R.: An upwind DG scheme preserving the maximum principle for the convective Cahn–Hilliard model. *Numer. Algorithms* **92**(3), 1589–1619 (2023)
3. Acosta-Soba, D., Guillén-González, F., Rodríguez-Galván, J.R., Wang, J.: Property-preserving numerical approximations of a Cahn–Hilliard–Navier–Stokes model with variable densities and degenerate mobility. *Appl. Numer. Math.* **209**, 68–83 (2025)
4. Altmann, R., Karsai, A., Schulze, P.: Structure-Preserving Discretization and Model Reduction for Energy-Based Models. *arXiv preprint arXiv:2507.21552* (2025)
5. Antonietti, P.F., Merlet, B., Pierre, M., Verani, M.: Convergence to equilibrium for a second-order time semi-discretization of the Cahn–Hilliard equation. *AIMS Math.* **1**(3), 178–194 (2016)

6. Bailo, R., Carrillo, J., Kalliadasis, S., Perez, S.: Unconditional bound-preserving and energy-dissipating finite-volume schemes for the Cahn–Hilliard equation. *Commun. Comput. Phys.* **34**(3), 713–748 (2023)
7. Bailo, R., Carrillo, J., Murakawa, H., Schmidtchen, M.: Convergence of a fully discrete and energy-dissipating finite-volume scheme for aggregation-diffusion equations. *Math. Models Methods Appl. Sci.* **30**, 2487–2522 (2020)
8. Barrett, J.W., Blowey, J.F., Garcke, H.: Finite element approximation of the Cahn–Hilliard equation with degenerate mobility. *SIAM J. Numer. Anal.* **37**(1), 286–318 (1999)
9. Bendimerad-Hohl, A., Haine, G., Matignon, D.: Structure-preserving discretization of the Cahn–Hilliard equations recast as a port-Hamiltonian system. In: International Conference on Geometric Science of Information, pp. 192–201. Springer (2023)
10. Boffi, D., Brezzi, F., Fortin, M.: Mixed Finite Element Methods and Applications. Springer (2013)
11. Brachet, M., Parnaudeau, P., Pierre, M.: Convergence to equilibrium for time and space discretizations of the Cahn–Hilliard equation. *Discrete Contin. Dyn. Syst. S* **15**(8), 1987 (2022)
12. Brunk, A., ten Eikelder, M.F.P.: A simple, fully-discrete, unconditionally energy-stable method for the two-phase Navier–Stokes Cahn–Hilliard model with arbitrary density ratios. *J. Comp. Phys.* **548**, 114558 (2026)
13. Brunk, A., Fritz, M.: Analysis and discretization of the Ohta–Kawasaki equation with forcing and degenerate mobility. *Partial Differ. Equ. Appl.* **6**, 54 (2025)
14. Brunk, A., Fritz, M.: Analysis and structure-preserving approximation of a Cahn–Hilliard–Forchheimer system with solution-dependent mass and volume source. *ESAIM Math. Model. Numer. Anal.* **59**(6), 2991–3020 (2025)
15. Brunk, A., Fritz, M.: Structure-Preserving Approximation of the Cahn–Hilliard–Biot System. *Numer. Methods Partial Differ. Equ.* **41**(1), e23159 (2025)
16. Chen, W., Du, X., Jing, J., Wu, H.: Optimal convergence of a fully decoupled finite difference scheme of the Abels–Garcke–Grün model for incompressible two-phase flows with unmatched densities. *Mathematics of Computation* (2025). DOI 10.1090/mcom/4140
17. Chen, W., Feng, W., Liu, Y., Wang, C., Wise, S.M.: A second order energy stable scheme for the Cahn–Hilliard–Hele–Shaw equations. *Discrete Contin. Dyn. Syst. B* **24**(1), 149–182 (2018)
18. Chen, W., Wang, S., Zhang, Y., Han, D., Wang, C., Wang, X.: Error estimate of a decoupled numerical scheme for the Cahn–Hilliard–Stokes–Darcy system. *IMA J. Numer. Anal.* **42**(3), 2621–2655 (2022)
19. Chu, H., Miyatake, Y., Cui, W., Wei, S., Furihata, D.: Structure-preserving physics-informed neural networks with energy or Lyapunov structure. In: Proceedings of the Thirty-Third International Joint Conference on Artificial Intelligence, pp. 3872–3880 (2024)
20. Diegel, A., Wang, C., Wang, X., Wise, S.: Convergence analysis and error estimates for a second order accurate finite element method for the Cahn–Hilliard–Navier–Stokes system. *Numer. Math.* **137**, 495–534 (2017)
21. Diegel, A.E., Feng, X.H., Wise, S.M.: Analysis of a mixed finite element method for a Cahn–Hilliard–Darcy–Stokes system. *SIAM J. Numer. Anal.* **53**(1), 127–152 (2015)
22. Ding, J., Ji, X.: A structure-preserving JKO scheme for the size-modified Poisson–Nernst–Planck–Cahn–Hilliard equations. *Numer. Math., Theory Methods Appl.* **16**(1), 204–229 (2023)
23. ten Eikelder, M.F.P.: A unified framework for N-phase Navier–Stokes Cahn–Hilliard Allen–Cahn mixture models with non-matching densities. *J. Fluid Mech.* **1013**, A26 (2025)
24. ten Eikelder, M.F.P., Khanwale, M.A.: Ostwald ripening and breakup characteristics of the advective Cahn–Hilliard equation: The role of free energy functionals. In: Proceedings of the Summer Program, Center for Turbulence Research, Stanford University, pp. 317–326 (2024)
25. ten Eikelder, M.F.P., Schillinger, D.: The divergence-free velocity formulation of the consistent Navier–Stokes Cahn–Hilliard model with non-matching densities, divergence-conforming discretization, and benchmarks. *J. Comput. Phys.* **513**, 113148 (2024)
26. ten Eikelder, M.F.P., Van Der Zee, K.G., Akkerman, I., Schillinger, D.: A unified framework for Navier–Stokes Cahn–Hilliard models with non-matching densities. *Math. Models Methods Appl. Sci.* **33**(01), 175–221 (2023)
27. Feng, X.: Fully Discrete Finite Element Approximations of the Navier–Stokes–Cahn–Hilliard Diffuse Interface Model for Two-Phase Fluid Flows. *SIAM J. Numer. Anal.* **44**, 1049–1072 (2006)

28. Feng, X., Wise, S.: Analysis of a Darcy–Cahn–Hilliard diffuse interface model for the Hele–Shaw flow and its fully discrete finite element approximation. *SIAM J. Numer. Anal.* **50**(3), 1320–1343 (2012)
29. Fritz, M.: Tumor evolution models of phase-field type with nonlocal effects and angiogenesis. *Bull. Math. Biol.* **85**(6), 44 (2023)
30. Fukao, T., Yoshikawa, S., Wada, S.: Structure-preserving finite difference schemes for the Cahn–Hilliard equation with dynamic boundary conditions in the one-dimensional case. *Commun. Pure Appl. Anal.* **16**(5), 1915–1938 (2017)
31. Giesselmann, J., Pryer, T.: Energy consistent discontinuous Galerkin methods for a quasi-incompressible diffuse two phase flow model. *ESAIM: Math. Model. Numer. Anal.* **49**(1), 275–301 (2015)
32. Gomez, H., Hughes, T.J.: Provably unconditionally stable, second-order time-accurate, mixed variational methods for phase-field models. *J. Comput. Phys.* **230**(13), 5310–5327 (2011)
33. Gonzalez, O.: Time integration and discrete Hamiltonian systems. *J. Nonlinear Sci.* **6**(5), 449–467 (1996)
34. Grün, G.: On convergent schemes for diffuse interface models for two-phase flow of incompressible fluids with general mass densities. *SIAM J. Numer. Anal.* **51**(6), 3036–3061 (2013)
35. Grün, G., Guillén-González, F., Metzger, S.: On fully decoupled, convergent schemes for diffuse interface models for two-phase flow with general mass densities. *Commun. Comput. Phys.* **19**(5), 1473–1502 (2016)
36. Grün, G., Klingbeil, F.: Two-phase flow with mass density contrast: stable schemes for a thermodynamic consistent and frame-indifferent diffuse-interface model. *J. Comput. Phys.* **257**, 708–725 (2014)
37. Guillén-González, F., Tierra, G.: Structure preserving finite element schemes for the Navier–Stokes–Cahn–Hilliard system with degenerate mobility. *Comput. Math. Appl.* **172**, 181–201 (2024)
38. Guillén-González, F., Tierra, G.: Second order schemes and time-step adaptivity for Allen–Cahn and Cahn–Hilliard models. *Comput. Math. Appl.* **68**(8), 821–846 (2014)
39. Guo, R., Xia, Y., Xu, Y.: An efficient fully-discrete local discontinuous Galerkin method for the Cahn–Hilliard–Hele–Shaw system. *J. Comput. Phys.* **264**, 23–40 (2014)
40. Han, D.: A decoupled unconditionally stable numerical scheme for the Cahn–Hilliard–Hele–Shaw system. *J. Sci. Comput.* **66**(3), 1102–1121 (2016)
41. Han, D., Wang, X.: A second order in time, decoupled, unconditionally stable numerical scheme for the Cahn–Hilliard–Darcy system. *J. Sci. Comput.* **77**(2), 1210–1233 (2018)
42. Hong, Q., Zhao, J., et al.: A physics-informed structure-preserving numerical scheme for the phase-field hydrodynamic model of ternary fluid flows. *Numer. Math. Theory Methods Appl.* **16**(3) (2023)
43. Huang, Q.A., Jiang, W., Yang, J.Z., Yuan, C.: A structure-preserving, upwind-SAV scheme for the degenerate Cahn–Hilliard equation with applications to simulating surface diffusion. *J. Sci. Comput.* **97**(3), 64 (2023)
44. Jüngel, A., Wang, B.: Structure-preserving semi-convex-splitting numerical scheme for a Cahn–Hilliard cross-diffusion system in lymphangiogenesis. *Math. Models Methods Appl. Sci.* **34**(10), 1905–1932 (2024)
45. Kay, D., Welford, R.: Efficient numerical solution of Cahn–Hilliard–Navier–Stokes fluids in 2D. *SIAM J. Sci. Comput.* **29**, 2241–2257 (2007)
46. Khanwale, M.A., Saurabh, K., Fernando, M., Calo, V.M., Sundar, H., Roszmanith, J.A., Ganapathysubramanian, B.: A fully-coupled framework for solving Cahn–Hilliard–Navier–Stokes equations: Second-order, energy-stable numerical methods on adaptive octree based meshes. *Comput. Phys. Commun.* **280**, 108501 (2022)
47. Kim, J., Lee, S., Choi, Y., Lee, S.M., Jeong, D.: Basic principles and practical applications of the Cahn–Hilliard equation. *Math. Probl. Eng.* **2016**(1), 9532608 (2016)
48. Kuang, B., Fu, H., Li, X.: Error estimates of linear decoupled structure-preserving incremental viscosity splitting methods for the Cahn–Hilliard–Navier–Stokes system. *arXiv preprint arXiv:2508.01141* (2025)
49. Li, M., Bi, J., Wang, N.: Structure-preserving weighted BDF2 methods for anisotropic Cahn–Hilliard model: Uniform/variable-time-steps. *Commun. Nonlinear Sci. Numer. Simul.* **140**, 108395 (2025)

50. McLachlan, R.I., Quispel, G.R.W., Robidoux, N.: Geometric integration using discrete gradients. *Phil. Trans. R. Soc. A* **357**(1754), 1021–1045 (1999)
51. Merlet, B., Pierre, M.: Convergence to equilibrium for the backward Euler scheme and applications. *Commun. Pure Appl. Anal.* **9**, 685–702 (2010)
52. Metzger, S.: An efficient and convergent finite element scheme for Cahn–Hilliard equations with dynamic boundary conditions. *SIAM J. Numer. Anal.* **59**(1), 219–248 (2021)
53. Metzger, S.: A convergent SAV scheme for Cahn–Hilliard equations with dynamic boundary conditions. *IMA J. Numer. Anal.* **43**(6), 3593–3627 (2023)
54. Metzger, S.: A convergent augmented SAV scheme for stochastic Cahn–Hilliard equations with dynamic boundary conditions describing contact line tension. *Interfaces Free Bound.* (2025)
55. Novick-Cohen, A.: The Cahn–Hilliard equation. *Handbook of Differential Equations: Evolutionary Equations* **4**, 201–228 (2008)
56. Okumura, M., Fukao, T.: Structure-preserving schemes for Cahn–Hilliard equations with dynamic boundary conditions. *Discrete Contin. Dyn. Syst. S* **17**(1), 362–394 (2024)
57. Okumura, M., Fukao, T., Furihata, D., Yoshikawa, S.: A second-order accurate structure-preserving scheme for the Cahn–Hilliard equation with a dynamic boundary condition. *Commun. Pure Appl. Anal.* **21**(2) (2022)
58. Qian, Y., Wang, C., Zhou, S.: Convergence analysis on a structure-preserving numerical scheme for the Poisson–Nernst–Planck–Cahn–Hilliard system. *CSIAM Trans. Appl. Math.* **4**(2) (2023)
59. Rybka, P., Hoffnlann, K.H.: Convergence of solutions to Cahn–Hilliard equation. *Commun. Partial Differ. Equ.* **24**(5–6), 1055–1077 (1999)
60. Schöberl, J.: C++11 implementation of finite elements in NGSolve. Tech. Rep. 30, ASC (Institute for Analysis and Scientific Computing) Report, TU Wien (2014)
61. Shen, J., Yang, X.: Numerical approximations of Allen–Cahn and Cahn–Hilliard equations. *Discrete Contin. Dyn. Syst. Ser. A* **28**(4), 1669–1691 (2010)
62. Shi, K., Su, H., Feng, X.: Structure-preserving and efficient numerical simulation for diffuse interface model of two-phase magnetohydrodynamics. *Phys. Fluids* **36**(8) (2024)
63. Shokrpour Roudbari, M., Şimşek, G., van Brummelen, E.H., van der Zee, K.G.: Diffuse-interface two-phase flow models with different densities: A new quasi-incompressible form and a linear energy-stable method. *Math. Models Methods Appl. Sci.* **28**(04), 733–770 (2018)
64. Tadmor, E., Miller, R., Elliott, R.: *Continuum Mechanics and Thermodynamics: From Fundamental Concepts to Governing Equations*. Cambridge University Press (2012)
65. Wang, B.: A structure-preserving quasi-convex-splitting finite-element scheme for a Cahn–Hilliard cross-diffusion system in lymphangiogenesis. *ESAIM: Math. Model. Numer. Anal.* **59**(3), 1685–1704 (2025)
66. Wang, Z., Lin, P., Yang, J.: Stability and error analysis of structure-preserving schemes for a diffuse-interface tumor growth model. *SIAM J. Sci. Comput.* **47**(1), B59–B86 (2025)
67. Wimmer, G.A., Southworth, B.S., Tang, Q.: A structure-preserving discontinuous Galerkin scheme for the Cahn–Hilliard equation including time adaptivity. *J. Comput. Phys.* p. 114097 (2025)
68. Wise, S.M.: Unconditionally stable finite difference, nonlinear multigrid simulation of the Cahn–Hilliard–Hele–Shaw system of equations. *J. Sci. Comput.* **44**(1), 38–68 (2010)
69. Wu, H.: A review on the Cahn–Hilliard equation: Classical results and recent advances in dynamic boundary conditions. *Electron. Res. Arch.* **30**(8), 2788–2832 (2022)
70. Yang, J., Kim, J.: An efficient stabilized multiple auxiliary variables method for the Cahn–Hilliard–Darcy two-phase flow system. *Comput. Fluids* **223**, 104948 (2021)
71. Yao, C., Zhang, F., Wang, C.: A scalar auxiliary variable (SAV) finite element numerical scheme for the Cahn–Hilliard–Hele–Shaw system with dynamic boundary conditions. *J. Comput. Math.* (2024)
72. Zhang, H., Wang, D., Wang, Z., Jia, H.: A decoupled finite element method for a modified Cahn–Hilliard–Hele–Shaw system. *AIMS Math.* **6**(8), 8681–8705 (2021)
73. Zheng, N., Li, X.: Error analysis of the SAV Fourier-spectral method for the Cahn–Hilliard–Hele–Shaw system. *Adv. Comput. Math.* **47**(5), 71 (2021)